ISSN: 0067-2904

photoconductive Detector Based on Graphene Doping with Silver Nanoparticles

Aya H. Mohammed[1], Asama N. Naje[1]*, Rawa k. Ibrahim[2]
[1]*Department of Physics, College of Science, University of Baghdad,*
[2]*Materials research dictorate, ministry of science and technology, Baghdad*

Received: 14/9/2021 Accepted: 2/3/2022 Published: 30/12/2022

Abstract

Graphene (Gr) decorated with silver nanoparticles (Ag NPs) were used to fabricate a wideband range photodetector. Silicon (Si) and porous silicon (PS) were used as a substrate to deposit Gr /Ag NPs by drop-casting technique. Silver nanoparticles (Ag NPs) were prepared using the chemical method. As well as the dispersion of silver NPs is achieved by a simple chemistry process on the surface of Gr.

The optical, structure and electrical characteristics of AgNPs and Gr decorated with Ag NPs were characterized by ultraviolet-visible spectroscopy (UV-Vis), x-ray diffraction (XRD). The X-ray diffraction (XRD) spectrum of Ag NPs exhibited 2θ values (38.1^o, 44.3^o, 64.5^o and 77.7^o) corresponding to the silver nanocrystal, while the XRD pattern of Gr-Ag NPs shows two distinct diffraction peaks at 2 θ = 26.2°and 54.7 which correspond to the (002), and (110). The absorption spectrum of Gr-AgNPs extended from UV to near IR region, surface plasmon resonance (SPR) absorption peak position for the AgNPs at (~320-480) nm. The I-V characteristics for the photoconductive detector on Si were measured with three sources: UV, visible, and IR. The photocurrent increased under the illumination of UV light (10W, 365nm), a Tungsten lamp (250W, 500-800nm), and a laser diode (300mW, 808nm). The I-V characteristics for the photoconductive detector on PS were measured with three sources: UV, Visible, and IR. Furthermore, we coated polyamide-nylon polymer on Gr/Ag NPs samples deposited on a Si and PS layer by the drop-casting method the results show that the photocurrent increased for all samples.

Keywords: sliver nanoparticles, Graphene, surface plasmon resonance, photoconductive detector, I-V Characteristics.

كاشف ضوئي يعتمد على تطعيم الجرافين مع جسيمات الفضة النانوية

آية حسن محمد[1] ، أسامة ناطق ناجي[1]* ، روى خليل ابراهيم[2]
[1]قسم الفيزياء، كلية العلوم، جامعة بغداد، بغداد، العراق
[2]دائرة بحوث المواد، وزارة العلوم و التكنولوجيا ،بغداد ،العراق

الخلاصة

*Email: oshumoma2000@gmail.com

تم استخدام الجرافين (Gr) المزين بجسيمات الفضة النانوية (Ag NPs) لتصنيع كاشف ضوئي واسع النطاق. تم استخدام السيليكون (Si) والسيليكون المسامي (PS) كركيزة لترسيب Gr / Ag NPs عن طريق تقنية الصب بالتنقيط. تم تحضير جسيمات الفضة النانوية (Ag NPs) باستخدام الطريقة الكيميائية. تم انجاز تشتت جسيمات الفضة النانوية على سطح Gr من خلال عملية كيميائية بسيطة.

تم دراسة الخصائص البصرية والتركيبية والكهربائية لـ AgNPs وGr المزينة بـ Ag NPs من خلال التحليل الطيفي المرئي فوق البنفسجي

(UV–Vis)، حيود الأشعة السينية (XRD). أظهر طيف حيود الأشعة السينية (XRD) لـ Ag NPs قيم 2θ (38.1°و 44.3°و 64.5 ° و77.7°) المقابلة للبلورة النانوية الفضية، بينما يُظهر نمط XRD لـ Gr–Ag NPs ذروتين حيود مميزين عند 2θ =26,2°و54.7° والتي

تتوافق مع (002) و (110). يمتد طيف الامتصاص لـ Gr–Ag NPs من منطقه فوق البنفسجية الى منطقه تحت الحمراء القريبة وموقع قمة

امتصاص رنين سطح البلازمون (SPR) لـ AgNPs عند (~ 320–480) نانومتر. تم قياس خصائص I–V للكاشف الضوئي على Si بثلاثة مصادر: الأشعة فوق البنفسجية والمرئية والأشعة تحت الحمراء. زاد التيار الضوئي تحت إضاءة ضوء الأشعة فوق البنفسجية (10 واط، 365 نانومتر)، مصباح التنغستن (250 واط، 500–800 نانومتر)، والصمام الثنائي ليزر (300 ميجا واط ، 808 نانومتر). تم قياس خصائص I–V للكاشف الضوئي على PS بثلاثة مصادر: الأشعة فوق البنفسجية والمرئية والأشعة تحت الحمراء.

علاوة على ذلك، قمنا بطلاء بوليمر نايلون بولي أميد على عينات Gr / Ag NPs المرسب على طبقة Si وPS، وأظهرت النتائج أن التيار الضوئي زاد لجميع العينات.

1. Introduction

Noble metal nanostructures are a type of functional material that has distinct physical and chemical properties that are influenced by its size, shape, composition, and structure [1,2]. The production of unique noble metal nanocrystals and their prospective applications in different sectors such as catalysis, electronics, sensing, and medicine have made significant progress [3–8]. Due to the scarcity and high cost of noble metals, combining them with other low-cost, sustainable materials is one of the most appealing approaches to improve their qualities and reduce their usage [9–11]. The resulting composition not only possesses the combined properties of their individual components but also potentially demonstrates novel functions with enhanced performance [12,13].

Noble metals have been successfully combined with inorganic nanostructures, organic molecules, polymers, biomaterials, and carbon materials, extending their prospective applications [9–15].

In metallic nanoparticles such as silver, the conduction band and the valence band are very close to each other as the electron moves freely. These free electrons give rise to the SPR absorption [16,17], occurring due to the collective oscillation of electrons of metal nanoparticles in resonance with the light wave [18]. Typically, the characteristic formation of colloidal silver nanoparticles is confirmed by the appearance of the sharp SPRs in the range of (350–600) nm [19, 20]. This absorption strongly depends on the particle size, the surrounding chemical and dielectric medium [17]. The UV-visible spectrum of the attenuated scattering of colloidal particles can be calculated from Mie theory [21]. Theoretically and experimentally, it is found that when size decreases, the SPR peak shifts towards the side of the shorter wavelength [22]. It was also found that with decreasing size, the absorption spectra become weak and broadband [22,23]. The same applies to the case of fluorescence [24-28].

The combination of noble metals and carbonaceous materials, such as carbon black and carbon nanotubes (CNTs), can improve the catalytic, electrochemical, and electrical characteristics of these materials dramatically [14,15]. Graphene has recently been employed as a promising foundation for the fabrication of graphene-based noble metal nanostructures [29,30].

The electrical and optical properties of graphene, a two-dimensional honeycomb lattice of carbon atoms, have piqued interest [31,32]. The unique characteristics stem from the zero-bandgap structure of graphene, which enables ultra-broadband optical applications from the ultraviolet to microwave regime [33]. In addition, graphene's higher carrier transfer properties enable the ultrafast operation of electronic and optical devices [34,35]. Moreover, the compatibility of graphene with developed complementary metal-oxide-semiconductor platforms has received considerable interest. Graphene-based low-cost, high-performance devices can be easily integrated on a single chip. Graphene-based photodetectors [36-41], optical modulators [42,43], and electronic circuits [44,45] have all been described using these features. Because of its high-speed functioning [37,39] and wide optical bandwidth [38], graphene has been widely used in photodetectors. However, the response of graphene photodetectors is limited to tens of mA/W due to the poor optical absorption of monolayer carbon atoms [41]. To improve the response of graphene photodetectors, various approaches have been proposed, including adsorption-supported lead sulfide quantum dots [46], graphene-semiconductor hybrid structures [19,20,47,48], and photonic nanostructures [40].

In this work first, have been focused on the synthesis of Ag NPs by chemical method, the prepared Ag NPs added to graphene. Graphene/Ag NPs nanocomposites was deposited on silicon and porous silicon to test it as a photoconductive detector in different spectrum regions.

2. MATERIALS AND METHODS

2.1 Synthesis of Silver Nanoparticles (AgNPs).

At first, silver nitrate solution had been prepared by dissolving 0.020 g of $AgNO_3$ in 100 mL distilled water. Then, $NaBH_4$ solution was prepared by dissolving 0.022 g of $NaBH_4$ in 200 mL distilled water. After that, solution of polyvinylpyrrolidone (PVP) was prepared by dissolving 0.1g of PVP in 30 mL of distilled water. Then, the synthesis of Ag NPs as in the following procedure: adding 30 mL of sodium borohydride ($NaBH_4$) to an Erlenmeyer flask. The liquid had been stirred and cooled at room temperature for about 20 minutes. Then dropped 2 mL of silver nitrate into the stirring $NaBH_4$ solution at approximately 1 drop per second. Initially, when to start to drop the $AgNO_3$; the liquid starts to seem yellow after two minutes, indicating the creation of silver nanoparticles. Finally, the PVP (poly N-vinyl pyrrolidone) was used as a protective medium for the silver nanoparticles' colloidal suspension. The PVP affects the molecular motion of reduced silver, inhibiting the aggregation of nanoparticles.

2.2 Synthesis of Gr-Ag Nanocomposite

Graphene solution was prepared by adding 0.05 g of Gr in 5 mL of distilled water. After 1h of sonication, the mixed solution was stirred for 3 days to form a homogeneous Gr suspension. Then, 1.2 ml of AgNPs solution was added into 4 ml from Gr with stirring for a week.

2.3 Preparation of Porous Silicon (PS) Layer by Electrochemical Etching (ECE)

Various PS production procedures have been proposed, as well as a variety of reaction mechanisms. The electrochemical etching procedure was used in this study. The electrochemical etching operation was carried out using the equipment depicted in Figure (1). Silicon wafers of the n-type (1.5 ×1.5 cm^2) were used, with an orientation of (111) and a low Resistivity of 0.02 Ohm-cm. To eliminate any remaining stains and debris, the wafers were cleaned numerous times with methanol and then with distilled water. Then dried in an oven, at 50ºC temperature.

After cleaning, the samples were immersed in a Teflon beaker containing 40% Hydrofluoric acid mixed with ethanol in a (1:1) ratio. The samples were placed vertically in the beaker on two Teflon tablets so that the etching current could complete the circuit between the top and bottom surfaces of the Si sample. The current density was set to 20 mA/cm^2, and the normal electrochemical etching period was set to 10 minutes. The nanostructure silicon films were used as a substrate for the manufacture of Photoconductive detector elements after the electrochemical etching process.

Figure 1: a) Cross section of anodization cell with ECE arrangement illustration and b) Teflon etching cell.

2.4 Fabrication of Photoconductive detector

A Si (n-type) wafer of (0.008-0.020) Ω.cm resistance and thickness of (525 ± 25μm) were used as a substrate for the photodetector. Samples with dimensions of 1.5 × 1.5 cm^2 were cut from a Si wafer and rinsed with distilled water and ethanol to remove dirt. An electrode spacing mask (0.4mm) was used to deposit aluminum electrodes on the Si surface, as shown in Figure (2).

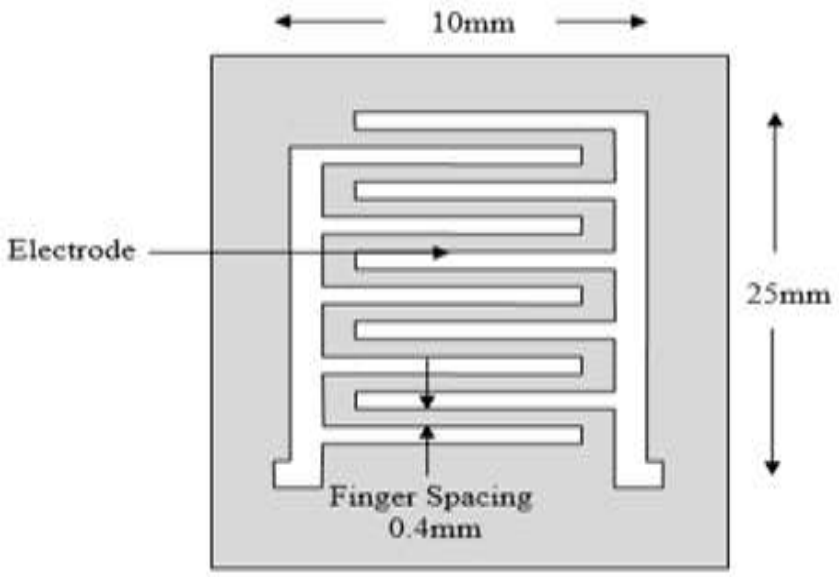

Figure 2: Schematic diagram for interdigital electrodes of photoconductive detector mask.

The Gr/Ag NPs solution was deposited on the electrodes by drop-casting technique, and the samples were left to dry at room temperature. The photodetector response is measured using ultraviolet light of wavelength and power (365 nm, 10 W), a tungsten lamp (500-800 nm, 250 W) and a laser diode (808 nm, 300 mW) as the illumination of the source. The measurement circuit of the photodetector is shown in Figure (3).

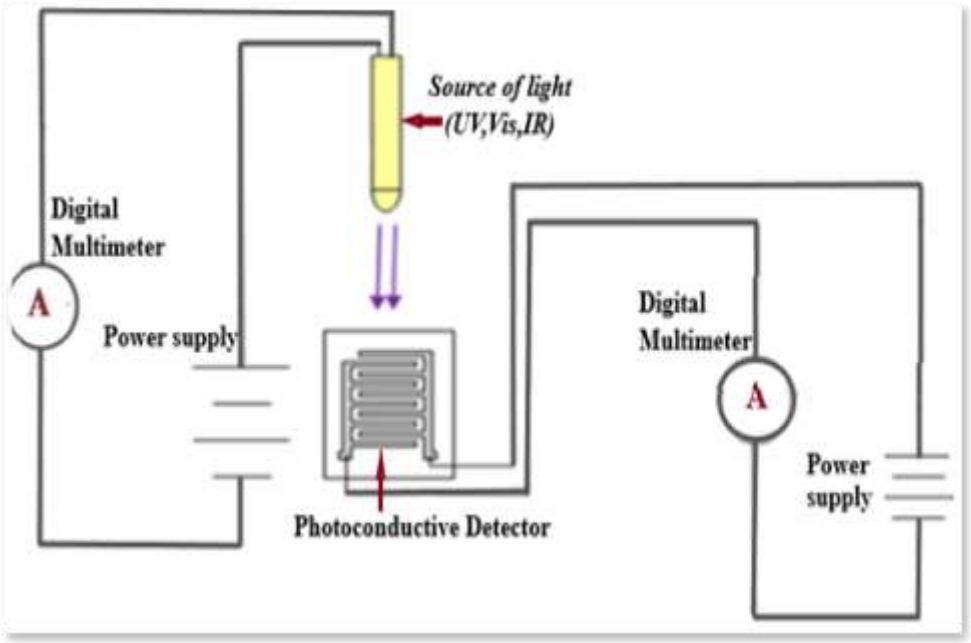

Figure 3: Schematic diagram of the experimental photoconductive detector setup.

3. Result and Discussion

3.1 UV-Vis spectroscopy analysis

The UV-Vis absorption spectra of the silver nanoparticles are shown in Figure (4a). The absorption (SPR) peak is obtained in the range of (~320–480) nm, no SPRs were observed at more than 500 nm, indicating that most of the AgNPs obtained have small sizes and similar

shapes. Such observation also gives preliminary indications regarding the size and size distribution of colloidal AgNPs.

Figure (4b) shows the ultraviolet-visible spectra of graphene. The spectrum of graphene has an absorption peak at 300 nm, which can be assigned to the n–π* transitions of C=O bonds [6,14]. Figure (4c) shows Optical properties in terms of absorbance and analysis of Gr-AgNPs were analyzed through UV-Vis spectrograph ranging from (200-1200) nm. Gr-AgNPs nanocomposites exhibited a plasmonic absorption band (~277) nm, indicating the presence of AgNPs in the Gr dispersion.

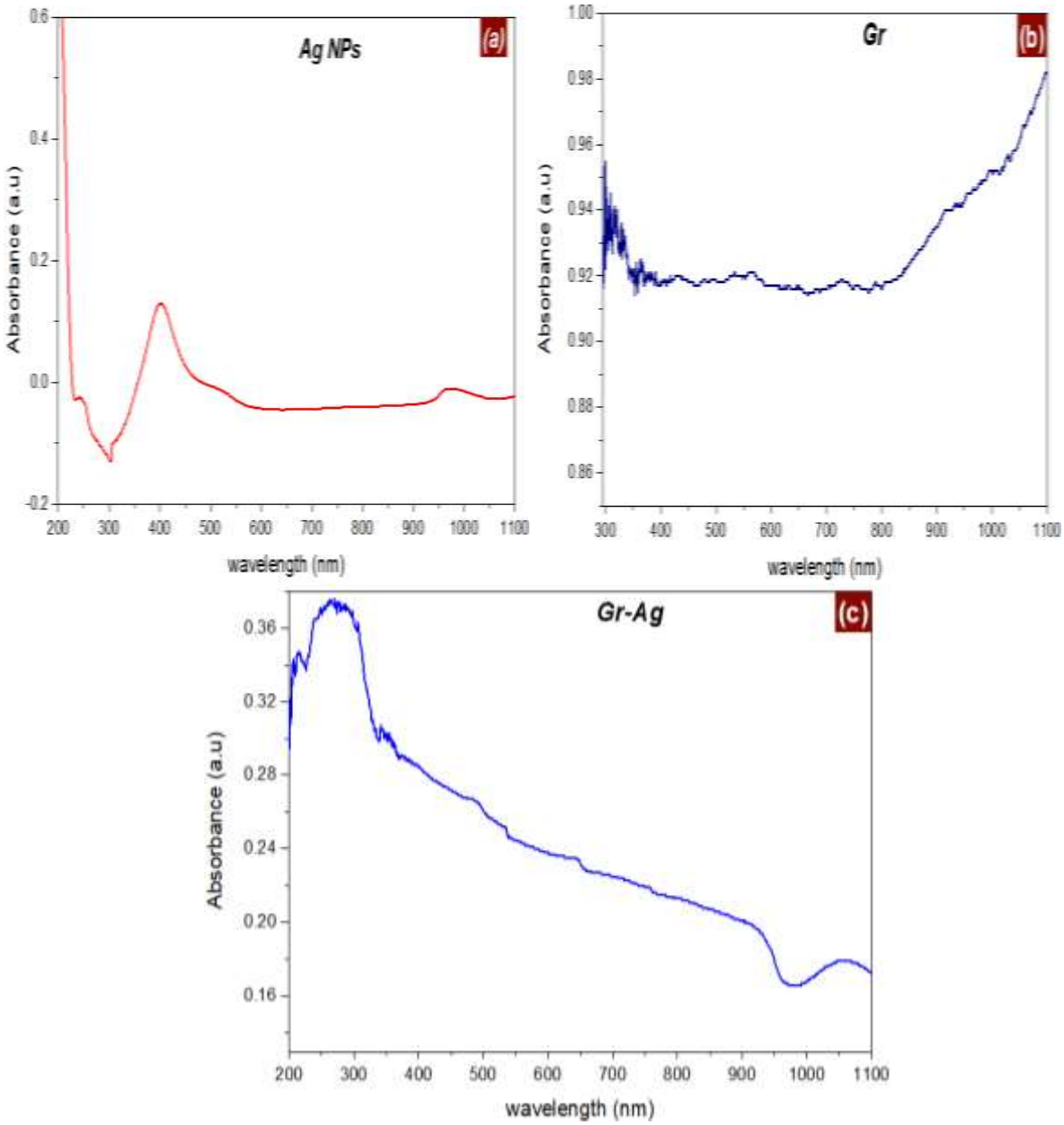

Figure 4: UV-Vis spectra of Ag-NPs, Gr and Gr-AgNPs.

3.2 XRD analysis

Figure (5) represents the XRD pattern of synthesized AgNPs, Gr and Gr-Ag nanocomposites. The prominent peaks of Ag nanoparticles, as well as Gr-Ag, were observed at 2θ values of 38.1°, 44.3 °, 64.5 ° and 77.7 °. These peaks are assigned for crystallographic

planes (1 1 1), (2 0 0), (2 2 0) and (3 1 1) of face-centered cubic (fcc) Ag nanoparticles. The corresponding d-spacing values of the Ag nanoparticles were investigated as (2.36, 2.04, 1.44 and 1.23) Å, respectively. The highest intense diffraction peak at around 38.1^{o} shows the pure crystalline nature of Ag nanoparticles [49]. As compared to Ag nanoparticles Gr-Ag shows two peaks at around 26.6° and 54.7° with d-spacing values of 3.327 and 1.671 A° correspond to the (002) and (110) planes, respectively.

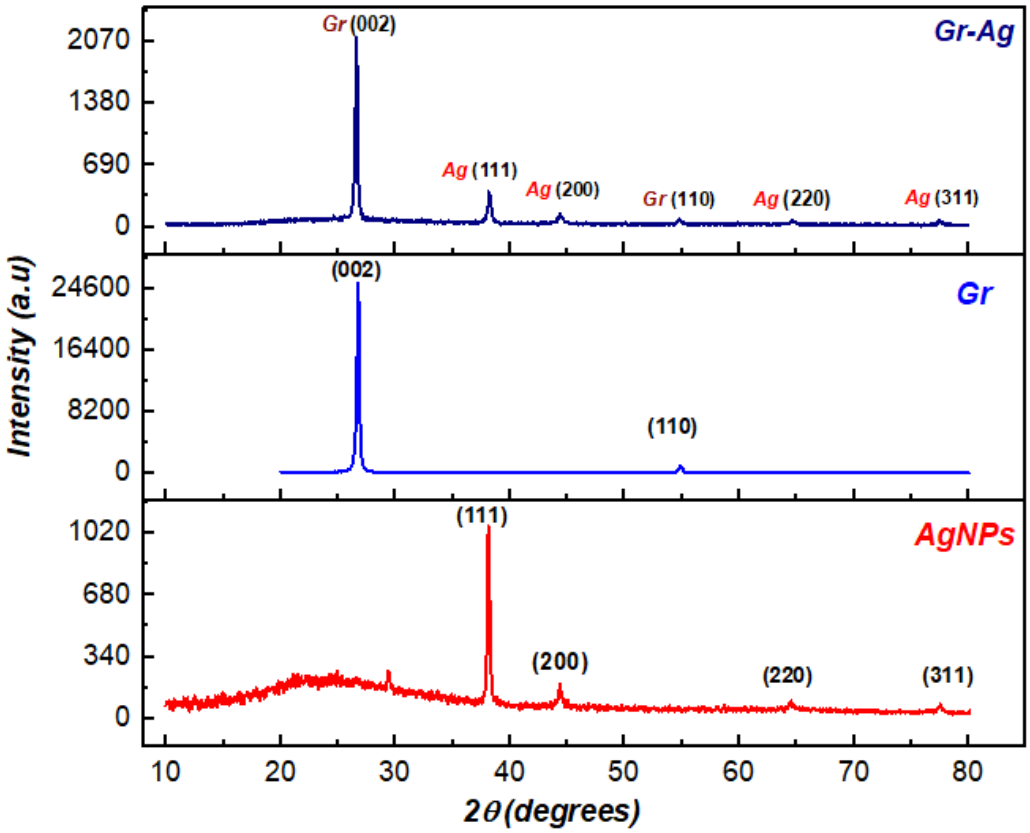

Figure 5: XRD patterns AgNPs, Gr and Gr-AgNPs nanocomposites.

3.3 Hall Effect Measurement

Hall effect experimental results can be used to interpret the conductivity type, Hall voltage, mobility, and carrier density parameters. The Hall measurements parameter for AgNPs, Gr-AgNPs/Si and Gr-Ag NPs/PS exhibit in Table (1)

Table 1: Hall Measurement parameter

Parameter	Charge Concentration (1/cm^3)	Conductivity (1/ Ω.cm)	Mobility (Cm^2/Vs)	Resistivity (Ω.cm)	Type
Ag NPs	1.08×10^{13}	2.36×10^{-1}	1.36×10^{5}	4.23	N-type
Gr/Ag NPs	3.073×10^{16}	$5\cdot874\times10^{-1}$	$1\cdot193\times10^{2}$	$1\cdot702$	P-type
Gr/Ag NPs/PS	$4\cdot731\times10^{15}$	$1\cdot807\times10^{-1}$	2.384×10^{2}	5.535	N-type

The table shows that the electrical conductivity of Gr/Ag NPs/Ps becomes much higher than that of Gr-AgNPs and Ag NPs and the concentration of carriers increases when Gr is

decorated with Ag NPs. The electrical transport of Gr-Ag NPs was improved when Gr was decorated with Ag NPs.

3.4 I-V Characteristics for photoconductive detector on silicon (Si) and porous silicon (PS) substrate

The current-voltage (I-V) characteristics of the manufactured photodetector are shown in Figure (6). The I-V curves in Figure (6(a) (b), (c), (d),(e) and (f)) indicate the ohmic nature of the detector. Using a tungsten lamp (250 W, 500-800 nm), ultraviolet light (10 W, 365 nm), and infrared light (300 mW, 808 nm) for illumination, it was observed that the light current under illumination had increased. The device is used up to 5V as the bias voltage and the corresponding current is shown in milliamperes. It can be seen that, the dark current is low in some regions, while the light current increases under illumination. The measurements of current in the dark and in illumination were studied as a function of voltage and presented in Figure (6 (a), (b), (c), (d), (e)and (f)).

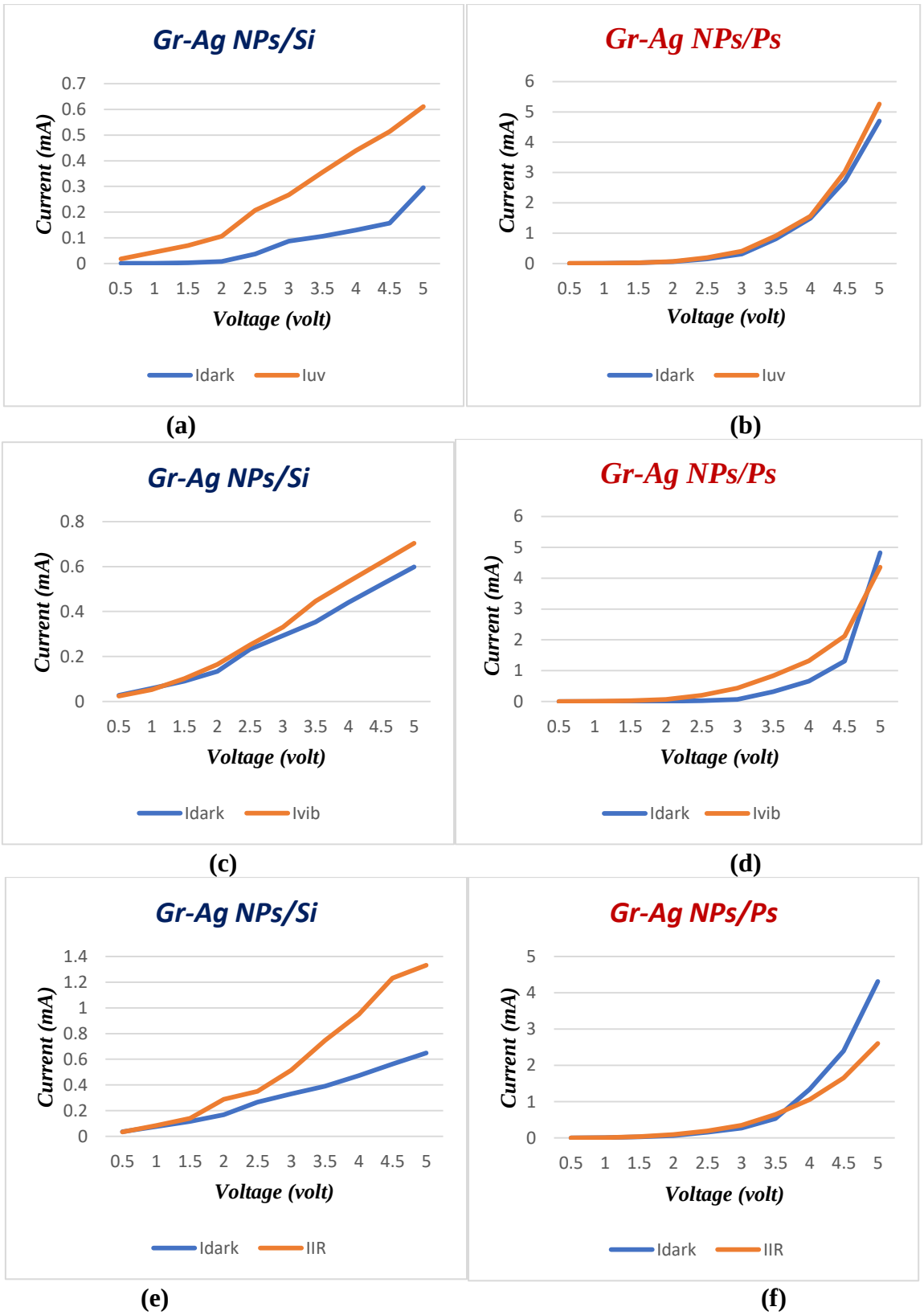

Figure 6: The variation of the (a) and (b)UV light, (c) and (d)Tungsten lamp (visible light), (e) and (f) Laser diode (IR) photocurrent of the fabrication photoconductive detector on Si and PS as a function of voltage for Gr-Ag NPs.

The figure of merit for a photoconductive detector for different sources of light (UV, Visible, and IR) have been shown in Table (2). At first, the photoconductive gain (G) has

been calculated, which is the ratio between the photocurrent to the dark current at the same bias voltage ($G=I_{ph}/I_D$). Also, the response time (τ) was calculated after calculating transit-time ($T_r=\ell^2/\mu.V_B$) which ℓ=0.4mm, V_B=5V and μ is the mobility for Gr/Ag NPs/Ps was found from Hall measurements, then by using the equation $G=\tau/T_r$ calculated response time in microsecond and then calculated noise equivalent power ($NEP= I_{noise}/R_\lambda$) where $I_{noise}= (2eI_{dark}\Delta f)^{1/2}$, Detectivity (D=1/NEP) and specific detectivity (D*=D(A Δf)½) where A represents the area of detector equal to 1cm^2 and Δf represent noise bandwidth equal to 1 Hz. It can be observed figure of merit for photoconductive detector from the table for Gr-Ag NPs/Si and Gr-AgNPs/PS.

Table 2: Figure of merit for photo-conductive detector as silicon and porous silicon substrate

Sample	*G*	*τ(μsec)*	*I_{noise} (A)*	*R_λ (A/Watt)*	*NEP (Watt)*	*D(Watt^{-1})*	*D(Watt^{-1}. Hz½.cm)*
UV light							
Gr/AgNPs/si	3.384	9.075	6.449×10^{-12}	0.044	1.465×10^{-10}	6.82×10^{9}	6.82×10^{9}
Gr/AgNPs/PS	1.043	1.399	$2 \cdot 18 \times 10^{-11}$	1.559×10^{-4}	1.398×10^{-7}	7.15×10^{6}	7.15×10^{6}
Tungsten lamp							
Gr/AgNPs/si	1.208	3.239	1.187×10^{-11}	2.132×10^{-3}	5.567×10^{-9}	1.79×10^{8}	1.79×10^{8}
Gr/AgNPs/PS	1.990	2.670	1.45×10^{-11}	5.28×10^{-6}	2.746×10^{-6}	3.64×10^{5}	3.64×10^{5}
Laser diode (808nm)							
Gr/AgNPs/si	2.008	5.385	1.230×10^{-11}	3.166	3.885×10^{-12}	2.57×10^{11}	2.57×10^{11}
Gr/AgNPs/PS	0.790	14.4	2.06×10^{-11}	3.53×10^{-3}	5.835×10^{-9}	1.71×10^{8}	1.71×10^{8}

After coated polyamide-nylon polymer on Gr-Ag NPS sample deposited on Si and PS layer by drop-casting method, the results show that the photocurrent increased for samples (Gr-Ag NPS/PS) and the polymer effect on it behave like Gr-Ag NPs with UV source, Visible source, and an infrared source. Whereas photocurrent of Gr-Ag NPS/Si layer samples is higher than without polymer, figure (7 a, b, c, d, e, and f) shows the variation of the photocurrent of the fabricated photoconductive detector on Si and PS layer with polymer and without polymer as a function of the bias voltage. This polymer coating can be considered as a surface treatment of the detector film, which highly increases the photoresponse and specific detectivity of the fabricated detector.

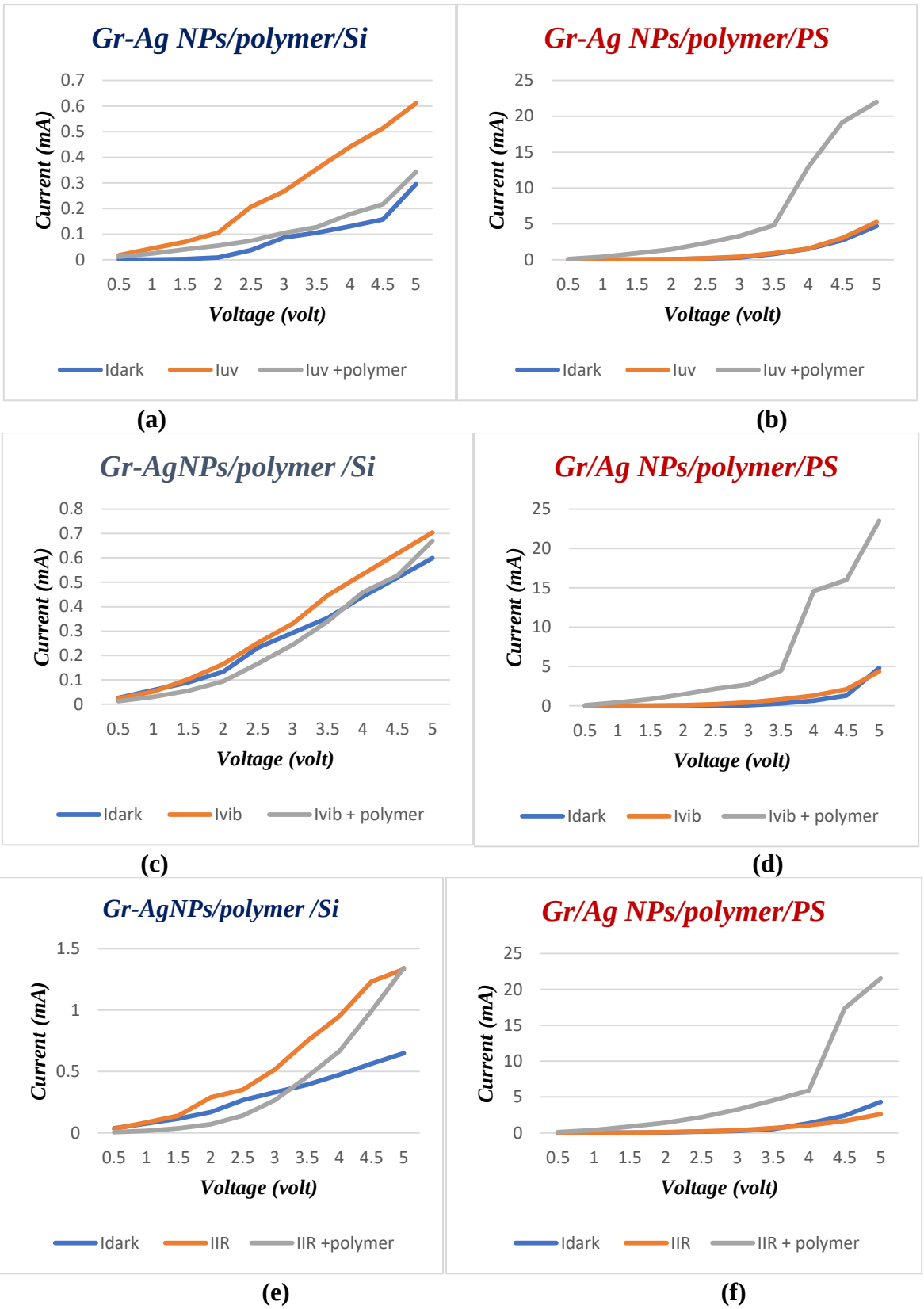

Figure 7: The variation of the (a) and (b) UV light, (c) and (d) Tungsten lamp (visible light), (e) and (f) Laser diode (IR) photocurrent of the fabrication photoconductive detector with coating polymer on Si and PS as a function of bias voltage for Gr-AgNPs/Polymer.

Conclusion

Photodetector Graphene decoration with silver nanoparticles synthesized by the chemical method was studied. The XRD, UV-visible spectra, hall effect and I-V Characteristics results were confirmed the property of the sample. It was found that, the nanoparticles were spatially well dispersed on the graphene. It is suggested that decorating the surface of Gr with Ag NPs can change the properties of materials from n-type to p-type. Experimental results showed that Gr-AgNPs can become important building blocks for photodetector synthesized on silicon (n-type), the device shows good response and response time for broadband wavelength especially Gr-Ag NPs.

References

[1] Daniel, Marie-Christine, and Didier Astruc., "Gold nanoparticles: assembly, supramolecular chemistry, quantum-size-related properties, and applications toward biology, catalysis, and nanotechnology.," *Chemical reviews,* vol. 104, pp. 293-346, 2004.

[2] ia, "Shape-controlled synthesis of metal nanocrystals: simple chemistry meets complex physics?," *Angew. Chem., Int. Ed.,* vol. 47, pp. 2-46, 2008.

[3] ng, X., Qi, X., Huang, Y., Li, S., Xue, C., Gan, C. L., ... & Zhang, H, "Photochemically controlled synthesis of anisotropic Au nanostructures: platelet-like Au nanorods and six-star Au nanoparticles," *ACS nano,* vol. 4, pp. 6196-6202, 2010.

[4] Andrea R., Jiaxing Huang, and Peidong Yang., "Langmuir− Blodgettry of nanocrystals and nanowires.," *Accounts of chemical research,* vol. 41, pp. 1662-1673., 2008.

[5] ray, Royce W., "Nanoelectrochemistry: metal nanoparticles, nanoelectrodes, and nanopores," *Chemical reviews,* vol. 108, pp. 2688-2720, 2008.

[6] , Shaojun, and Erkang Wang, "Noble metal nanomaterials: controllable synthesis and application in fuel cells and analytical sensors.," *Nano Today* , vol. 6, no. 3, pp. 240-264, 2011.

[7] s, Matthew R., et al. , "Templated techniques for the synthesis and assembly of plasmonic nanostructures.," *Chemical reviews,* vol. 111, no. 6, pp. 3736-3827, 2011.

[8] ey, Claire M., et al, "Gold nanostructures: a class of multifunctional materials for biomedical applications.," *Chemical Society Reviews* , vol. 40, no. 1, pp. 44-56, 2011.

[9] S., Fan, C., Wu, T., & Anderson, S. L, "CO oxidation on Au n/TiO2 catalysts produced by size-selected cluster deposition," *Journal of the American Chemical Society* , vol. 126, no. 18, pp. 5682-5683, 2004.

[10] Yadong, and A. Paul Alivisatos, "Colloidal nanocrystal synthesis and the organic–inorganic interface." Nature 437.7059 (2005): 664-670.Colloidal nanocrystal synthesis and the organic–inorganic interface," *Nature,* vol. 437, pp. 664-670, 2005.

[11] KM Kerry, Connie MY Yeung, and Shik Chi Tsang., "Carbon dioxide fixation into chemicals (methyl formate) at high yields by surface coupling over a Pd/Cu/ZnO nanocatalyst," *Journal of the American Chemical Society* , vol. 129, no. 20, pp. 6360-6361, 2007.

[12] ., Lu, G., Zhou, X., Cao, X., Boey, F., & Zhang, H, "Controlled assembly of gold nanoparticles and graphene oxide sheets on dip pen nanolithography-generated templates," *Langmuir* , vol. 25, no. 18, pp. 10455-10458, 2009.

[13] ı, W., Du, G., Hu, P., Yin, Y., Li, J., Yu, J., ... & Zhang, H, "Nanopaper based on Ag/TiO2 nanobelts heterostructure for continuous-flow photocatalytic treatment of liquid and gas phase pollutants," *Journal of hazardous materials* , vol. 197, pp. 19-25, 2011.

[14] uan Z., Xiaozhu Z., Xiao H.,Zhijuan W., Yanli Y., Qichun Z., Freddy B. and Hua Z., "Electrochemical deposition of Pt nanoparticles on carbon nanotube patterns for glucose detection," *Analyst,* vol. 135, no. 7, pp. 1726-1730, 2010.

[15] ; Li, Chin Foo Goh, Xiaozhu Zhou, Gang Lu, Hosea Tantang, Yanhong Chen, Can Xue, Freddy Y. C. Boey,and Hua Z., "Patterning colloidal metal nanoparticles for controlled growth of carbon

nanotubes," *Advanced Materials* , vol. 20, no. 24, pp. 4873-4878, 2008.

[16] ıg, Xiao, et al. , "Graphene-based composites," *Chemical Society Reviews,* vol. 41, no. 2, pp. 666-686, 2012.

[17] ı H., Zongyou Y., Shixin W., Xiaoying Q., Qiyuan H., Qichun Z., Qingyu Y., Freddy B., and Hua Z., "Graphene-based materials: synthesis, characterization, properties, and applications," *small* , vol. 7, no. 14, pp. 1876-1902, 2011.

[18] n, A.K.; Novoselov, K.S. , "The rise of graphene," *Nat. Mater.*, vol. 6, p. 183–191, 2007.

[19] Novoselov, K.S.; Fal'Ko, V.I.; Colombo, L.; Gellert, P.R.; Schwab, M.G.; Kim, K. , "A roadmap for graphene," *Nature* , vol. 490, no. 192–200, 2012.

[20] ıccorso, F.; Sun, Z.; Hasan, T.; Ferrari, A.C. , "Graphene photonics and optoelectronics," *Nat. Photonics* , vol. 4, p. 611–622, 2010.

[21] Ni, G.X.; Wang, L.; Goldflam, M.D.; Wagner, M.; Fei, Z.; McLeod, A.S.; Liu, M.K.; Keilmann, F.; Özyilmaz, B.; Castro Neto, A.H.; et al. , "Ultrafast optical switching of infrared plasmon polaritons in high-mobility graphene," *Nat. Photonics* , vol. 10, p. 244–247, 2016.

[22] Kim, S.; Nah, J.; Jo, I.; Shahrjerdi, D.; Colombo, L.; Yao, Z.; Tutuc, E.; Banerjee, S.K. , "Realization of a high mobility dual-gated graphene field-effect transistor with Al2O3 dielectric. 2009, 94.," *Appl. Phys. Lett.* , vol. 94, 2009.

[23] ıg, K.E.; Yoo, T.J.; Kim, C.; Kim, Y.J.; Lee, S.K.; Kim, S.-Y.; Heo, S.; Kwon, M.G.; Lee, B.H., "Gate-controlled graphene–silicon schottky junction photodetector," *Small* , vol. 14, no. 28, p. 1801182, 2018.

[24] ller, T.; Xia, F.; Avouris, P. , "Graphene photodetectors for high-speed optical communications," *Nat. Photonics* , vol. 4, p. 297–301, 2010.

[25] C.H.; Chang, Y.C.; Norris, T.B.; Zhong, Z. , "Graphene photodetectors with ultra-broadband and high responsivity at room temperature," *Nat. Nanotechnol* , vol. 9, p. 273–278, 2014.

[26] X.; Shiue, R.J.; Gao, Y.; Meric, I.; Heinz, T.F.; Shepard, K.; Hone, J.; Assefa, S.; Englund, D., "Chip-integrated ultrafast graphene photodetector with high responsivity," *Nat. Photonics* , vol. 7, p. 883–887, 2013.

[27] nakyapan, S.; Lu, P.K.; Navabi, A.; Jarrahi, M. , "Gold-patched graphene nano-stripes for high-responsivity and ultrafast photodetection from the visible to infrared regime. Light. Sci. Appl. 2018, 7," *Light. Sci. Appl.*, vol. 7, no. 1, pp. 1-9, 2018.

[28] F.; Mueller, T.; Lin, Y.M.; Valdes-Garcia, A.; Avouris, P. , "Ultrafast graphene photodetector," *Nat. Nanotechnol*, vol. 4, no. 12, pp. 839-843, 2009.

[29] ınello, V.; Midrio, M.; Contestabile, G.; Asselberghs, I.; Van Campenhout, J.; Huyghebaert, C.; Goykhman, I.; Ott, A.K.; Ferrari, A.C.; Romagnoli, M. , "Graphene-silicon phase modulators with gigahertz bandwidth," *Nat. Photonics* , vol. 12, no. 1, pp. 40-44, 2018.

[30] M.; Yin, X.; Ulin-Avila, E.; Geng, B.; Zentgraf, T.; Ju, L.; Wang, F.; Zhang, X. , "A graphene-based broadband optical modulator," *Nature* , vol. 474, no. 7349, pp. 64-67, 2011.

[31] Y.; Lin, Y.M.; Bol, A.A.; Jenkins, K.A.; Xia, F.; Farmer, D.B.; Zhu, Y.; Avouris, P., "High-frequency, scaled graphene transistors on diamond-like carbon," *Nature* , vol. 472, no. 7341, pp. 74-78, 2011.

[32] vierz, Frank., "Graphene transistors," *Nature nanotechnology* , vol. 5, no. 7, pp. 487-496, 2010.

[33] ısimos K., Michela B,, Louis G., Johann O., Maria B., F. Pelayo Garcia de Arquer, Fabio G. & Frank H. L. Koppens, "Hybrid graphene–quantum dot phototransistors with ultrahigh gain," *Nature nanotechnology,* vol. 7, no. 6, pp. 363-368, 2012.

[34] ı, H.; Yuan, J.; Xu, Z.; Chen, C.; Lin, S.; Wang, Y.; Song, J.; Liu, Y.; Khan, Q.; Hoh, H.Y.; et al., "Broadband photodetectors based on graphene–Bi2Te3 heterostructure," *Acs Nano,* vol. 9, no. 2, pp. 1886-1894, 2015.

[35] K., Padmanabhan, M., Goswami, S., Sai, T. P., Ramalingam, G., Raghavan, S., & Ghosh, A., "Graphene–MoS 2 hybrid structures for multifunctional photoresponsive memory devices," *Nature nanotechnology* , vol. 8, no. 11, pp. 826-830, 2013.

[36] hong A., Fangze L., Yung J.J., and Swastik K., "Tunable graphene–silicon heterojunctions for ultrasensitive photodetection," *Nano letters,* vol. 13, no. 3, pp. 909-916, 2013.

[37] ze L. and Swastik K., "Quantum carrier reinvestment-induced ultrahigh and broadband photocurrent responses in graphene–silicon junctions," *ACS nano* , vol. 8, no. 10, pp. 10270-10279, 2014.

[38] aleb, C. Petit, and M. P. Pileni, "Optical properties of self-assembled 2D and 3D superlattices of silver nanoparticles," *The Journal of Physical Chemistry B,* vol. 102, no. 12, pp. 2214-2220, 1998.

[39] . Noginov, G. Zhu, M. Bahoura, J. Adegoke, C. Small, B.A. Ritzo, V.P. Drachev & V.M. Shalaev, "The effect of gain and absorption on surface plasmons in metal nanoparticles," *Applied Physics B* , vol. 86, no. 3, pp. 455-460, 2007.

[40] Nath, D. Chakdar, and G. Gope,, "Synthesis of CdS and ZnS Quantum Dots and Their Applications in Electronics," *Nanotrends: J. Nanotechnol. App.* , vol. 2, pp. 1-3, 2007.

[41] Pileni, "Optical properties of nanosized particles dispersed in colloidal solutions or arranged in 2D or 3D superlattices," *New J. Chem.* , vol. 22, p. 693–702, 1998.

[42] M.M. Alvarez, J.T. Khoury, T.G. Schaaff, M.N. Shafigullin, I. Vezmar, and R.L. Whetten, "Optical absorption spectra of nanocrystal gold molecules," *J. Phys. Chem. B* , vol. 101, p. 1997, 3706–3712.

[43] ink and M.A. El-Sayed, "Shape and size dependence of radiative, non-radiative and photothermal properties of gold nanocrystals," *Int. Rev. Phys. Chem.* , vol. 19, p. 409–453, 2000.

[44] reguer, F. Rocco, G. Lelong, A.L. Nestour, T. Cardinal, A. Maali, and B. Lounis, "Fluorescence silver oligomeric cluster and colloidal particles," *Solid State Sci.* , vol. 7, no. 7, pp. 812-81, 2005.

[45] ouheiler, M.R. Beversluis, and L. Novonty, "Characterization of nano plasmonics structures by locally excited photoluminescences," *Applied physics letters,* vol. 83, no. 24, pp. 5041-5043, 2003.

[46] le, S., Deshpande, A. C., Singh, S. B., & Kulkarni, S. K, "Tuning luminescence intensity of RHO6G dye using silver nanoparticles," *Bulletin of Materials Science 31.3 (2008):* , vol. 31, no. 3, pp. 541-544, 2008.

[47] Drachev, E.N. Khaliullin, W. Kim, F. Alzoubi, S.G. Rautian, V.P. Safonov, R.L. Armstrong, and V.M. Shalaev, "Quantum size effect in two-photon excited luminescence from silver nanoparticles," *Phys. Rev. B: Condens. Matter* , vol. 69, no. 3, p. 035318–035323, 2004.

[48] Siwach and P. Sen, "Synthesis and study of fluorescence properties of Cu nanoparticles," *J. Nanopart. Res.,* vol. 10, p. 107–114., 2008.

[49] . Das, R. K. Sharma, R. Saikia, V. S. Kale, M. V. Shelke, and P. Sengupta, "Synthesis of silver nanoparticles in an aqueous suspension of graphene oxide sheets and its antimicrobial activit," *Colloids and Surfaces B: Biointerfaces,* vol. 83, no. 1, pp. 16-22, 2011.

[50] . T. W. M. Y. K. B. M. M. a. F. U. D. Afarin B., "Low temperature hall effect investigation of conducting polymer-carbon nanotubes composite network," *International journal of molecular sciences* , vol. 13, no. 11, pp. 14917-14928, 2012.